

ORIGINAL ARTICLE

ATP-induced cellular stress and mitochondrial toxicity in cells expressing purinergic P2X7 receptor

Swen Seeland^{1,2}, H el ene Kettiger³, Mark Murphy¹, Alexander Treiber¹, Jasmin Giller¹, Andrea Kiss¹, Romain Sube¹, Stephan Kr ahenb uhl⁴, Mathias Hafner² & J org Huwyler³

¹Actelion Pharmaceuticals Ltd, Gewerbestrasse 16, 4123 Allschwil, Switzerland

²Institute for Molecular and Cell Biology, University of Applied Science, Paul-Wittsack-Strasse 10, 68163 Mannheim, Germany

³Division of Pharmaceutical Technology, Department of Pharmaceutical Sciences, University of Basel, Klingelbergstrasse 50, 4056 Basel, Switzerland

⁴Division of Clinical Pharmacology and Toxicology, University Hospital of Basel, 4056 Basel, Switzerland

Keywords

Cytosensor, extracellular adenosine triphosphate (ATP), metabolic stress, mitochondrial toxicity, P2X7, purinergic receptor

Correspondence

J org Huwyler, Division of Pharmaceutical Technology, Department of Pharmaceutical Sciences, University of Basel, Klingelbergstrasse 50, CH-4056 Basel, Switzerland. Tel: + 41 61 267 15 13; Fax: + 41 61 267 15 16; E-mail: joerg.huwyler@unibas.ch

Funding Information

This project was supported by grants from the Swiss Centre of Applied Human Toxicology (SCAHT) and the "Freie Akademische Gesellschaft Basel" (FAG).

Received: 8 October 2014; Revised: 10 December 2014; Accepted: 19 December 2014

Pharma Res Per, 3(2), 2015, e00123, doi: 10.1002/prp2.123

doi: 10.1002/prp2.123

Abstract

Under pathological conditions, the purinergic P2X7 receptor is activated by elevated concentrations of extracellular ATP. Thereby, the receptor forms a slowly dilating pore, allowing cations and, upon prolonged stimulation, large molecules to enter the cell. This process has a strong impact on cell signaling, metabolism, and viability. This study aimed to establish a link between gradual P2X7 activation and pharmacological endpoints including oxidative stress, hydrogen peroxide generation, and cytotoxicity. Mechanisms of cellular stress and cytotoxicity were studied in P2X7-transfected HEK293 cells. We performed real-time monitoring of metabolic and respiratory activity of cells expressing the P2X7-receptor protein using a cytosensor system. Agonistic effects were monitored using exogenously applied ATP or the stable analogue BzATP. Oxidative stress induced by ATP or BzATP in target cells was monitored by hydrogen peroxide release in human mononuclear blood cells. P2X7-receptor activation was studied by patch-clamp experiments using a primary mouse microglia cell line. Stimulation of the P2X7 receptor leads to ion influx, metabolic activation of target cells, and ultimately cytotoxicity. Conversion of the P2X7 receptor from a small cation channel to a large pore occurring under prolonged stimulation can be monitored in real time covering a time frame of milliseconds to hours. Selectivity of the effects can be demonstrated using the selective P2X7-receptor antagonist AZD9056. Our findings established a direct link between P2X7-receptor activation by extracellular ATP or BzATP and cellular events culminating in cytotoxicity. Mechanisms of toxicity include metabolic and oxidative stress, increase in intracellular calcium concentration and disturbance of mitochondrial membrane potential. Mitochondrial toxicity is suggested to be a key event leading to cell death.

Abbreviations

1321N1, human astrocytoma cell line; AZD9056, P2X7-receptor antagonist; BzATP, 2', 3'-O-(4-benzoylbenzoyl)-ATP; HEK293, human embryonic kidney cells 293; HEK-hP2X7, human embryonic kidney cells 293 overexpressing P2X7; JC-1, 5,5',6,6'-tetrachloro-1,1',3,3'-tetraethylbenzimidazolylcarbocyanine iodide; MAPK, mitogen-activated protein kinase; P2X7, purinergic receptor P2X, ligand-gated ion channel 7; YoPro1, 4-[(Z)-(3-methyl-1,3-benzoxazol-2(3H)-ylidene)methyl]-1-[3-(trimethylammonio)propyl]quinolinium diiodide.

Introduction

Adenosine triphosphate (ATP) plays a central role in cell metabolism. Intracellular concentrations of ATP range from 1 to 10 mmol/L (Beis and Newsholme 1975). Extracellular ATP concentrations are regulated by ATPases (Burnstock 2006), and are typically very low under physiological conditions. There are, however, conditions in which local extracellular ATP concentrations reach high levels (Volonte *et al.* 2003; Burnstock 2006). For example, ATP is released at the synapses of neurons, where it acts as a neurotransmitter (Bardoni *et al.* 1997; Pankratov *et al.* 2006). In addition, intracellular ATP is released into the extracellular space in conditions of cell necrosis or hypoxia (Billingsley *et al.* 2004; Rousseau *et al.* 2004; Sharnez *et al.* 2004; Schroder and Tschopp 2010). Moreover, prolonged stimulation with ATP induces cell death in leukocytes and endothelial cells (Dawicki *et al.* 1997; Yoon *et al.* 2006; Cosentino *et al.* 2011). These extreme effects occurring at extracellular ATP concentrations above 500 $\mu\text{mol/L}$ are thought to be induced, in part, by the purinergic receptor P2X7 (Chessell *et al.* 1998; Arbeloa *et al.* 2012). Such ATP concentrations are more than 10 times higher than those required for activation of other P2X or P2Y receptors. Sustained exposure (>1 min) to ATP levels above 500 $\mu\text{mol/L}$ enables the P2X7 receptor to form a large, nonselective pore, which allows molecules of up to 900 Da to enter the cell (Surprenant 1996). Prolonged opening of the P2X7 pore initiates several events with serious consequences for the cells, including cell death (Buisman *et al.* 1988; Ferrari *et al.* 1997; Labasi *et al.* 2002).

Mechanistic studies indicated that activation of the P2X7 receptor leads to a distinct sequence of events (North 2002). Electrophysiological studies have shown that opening of an ion channel selective for small cations (Na^+ , K^+ , and Ca^{2+}) occurs within the first milliseconds of stimulation. After several seconds, permeability for larger organic cations increases progressively, with maximum dilatation of the ion channel reached after several minutes. However, the underlying molecular mechanisms of this process remain still unclear (North 2002).

Activation of the P2X7 receptor initiates a series of cellular responses that include depolarization, activation of phospholipase C, and a rise in intracellular Ca^{2+} concentrations, which stimulates caspase-1 activity, cytokine release, and activation of p38 mitogen-activated protein kinase (MAPK) (Armstrong *et al.* 2002; Ferrari *et al.* 2006; Donnelly-Roberts *et al.* 2009). Furthermore, activation of P2X7 leads to recruitment, binding and activation of additional channel-forming proteins, namely, the glycoprotein pannexin 1 (Locovei *et al.* 2007). Such events, in turn, have a plethora of effects. For example, cytokine signaling provokes an inflammatory stimulus in cells of

the immune system (Volonte *et al.* 2012). Some of these events are pathologically important, for example, in neurodegeneration (Takenouchi *et al.* 2010), tumor growth (Ryu *et al.* 2011), and kidney disease (Birch *et al.* 2013). In transgenic mice, disruption of P2X7-receptor function has a detrimental impact on adipogenesis and lipid metabolism, pointing to an important physiological role of P2X7 in energy metabolism (Beaucage *et al.* 2013). Consequently, several P2X7 antagonists have been developed in recent years (Chrovian *et al.* 2014). One of these compounds is the selective P2X7-receptor antagonist AZD9056 (Bhattacharya *et al.* 2011) whose efficacy in rheumatoid arthritis was evaluated in a phase II clinical trials (Keystone *et al.* 2012).

While many of the above-mentioned phenomena have been extensively characterized, their link to P2X7 activity has not been conclusively shown. In particular, it is difficult to monitor gradual activation of the P2X7 receptor on a time scale ranging from a few milliseconds up to minutes or hours. Thus, the present project aimed to study the dynamics of P2X7-receptor activation, using a P2X7-expressing mouse microglia cell line (BV2) and a recombinant human HEK293 cell line overexpressing P2X7 (HEK-hP2X7). To this end, we linked pharmacological endpoints, such as cytotoxicity or hydrogen peroxide (H_2O_2) release as an indicator of oxidative stress, to P2X7-receptor activation, altered ion flow, disturbance of membrane potential, cellular metabolism, and respiration. In this study, we used well-known and established cell systems and additional recently developed HEK-hP2X7 cells for comparisons and conformational reasons of the performed assays. Real-time monitoring of metabolic and respiratory activity of P2X7-expressing cells was achieved using a novel cytosensor system (Seeland *et al.* 2013). This cell-based cytosensor system allows real-time monitoring of metabolic activity (pH changes), respiration (oxygen consumption), as well as cellular morphology and adhesion of cells (Thedinga *et al.* 2007).

Materials and Methods

Chemicals

ATP and BzATP were purchased from Sigma (Buchs, Switzerland), dissolved in water, and adjusted to pH 7.4 using sodium hydroxide. Fluo-4 acetoxymethyl ester (Fluo-4-AM) was obtained from Life Technologies (Basel, Switzerland). The cyanine dye JC-1 (5,5',6,6'-tetrachloro-1,1',3,3'-tetraethylbenzimidazolylcarbocyanine iodide) was obtained from Enzo Life Sciences (Lausen, Switzerland). Valinomycin was obtained from Sigma-Aldrich (St. Louis, MO). All other chemicals were of analytical quality. The P2X7-receptor antagonist AZD9056 (Bhattacharya

et al. 2011) was used as a stock solution in dimethyl sulfoxide (DMSO). Final DMSO concentrations in experiments did not exceed 1.0% (v/v). As demonstrated by control incubations, these DMSO concentrations were not cytotoxic and did not interfere with the assays. The CellTiter-Blue cell viability assay was obtained from Promega (Dübendorf, Switzerland).

Preparation of mononuclear blood cells (lymphocytes, monocytes, and macrophages)

For the preparation of fresh mononuclear cells, 30 mL of male human blood containing 10% (v/v) sodium citrate as anticoagulant was collected, and mononuclear cells were isolated by Polymorphprep™ (Axis-Shield, Oslo, Norway) density centrifugation according to the manufacturer's protocol. Briefly, 15 mL of human blood was layered on 17 mL of Polymorphprep buffer (Axis-Shield) in a 50 mL reaction tube and centrifuged at 500g for 30 min at 22°C. The resulting mononuclear cell band was transferred to a new 50 mL reaction tube and diluted with one equivalent of aqueous sodium chloride solution (0.45%, v/v) to restore physiological osmolarity. The solution was centrifuged at 450g for 18 min at 20°C and the supernatant removed. Subsequently, the cell pellet was reconstituted in 0.9% (w/v) aqueous sodium chloride solution and again centrifuged at 400g for 10 min at 20°C. The supernatant was removed, and remaining red blood cells were hypertonically lysed by adding 9 mL of demineralized water for 17 sec, and then centrifuged at 300g for 10 min at 20°C. The cell pellet obtained in the last centrifugation step was reconstituted in 20 mL of phosphate-buffered saline (PBS), and cell viability and concentration were analyzed using a Vi-cell XR cell viability analyzer (Beckman Coulter, Krefeld, Germany). Cell concentration was adjusted to 2×10^6 cells/mL, and a 250 μ L aliquot of this cell suspension was dispensed into a 96-well plate and immediately used for experiments.

Human astrocytoma 1321N1 cells

Human astrocytoma 1321N1 cells were stably transfected with the human receptors P2X1, P2X2, P2X3, P2X4, or P2X7 and individual clones were subsequently picked and cultivated for further experiments. Human astrocytoma 1321N1 cells were cultured under standard cell culture conditions in Dulbecco's modified Eagle medium (DMEM) with 2.0 mmol/L GlutaMAX (Life Technologies) supplemented with 50 IU/mL penicillin, 50 μ g/mL streptomycin, and 10% (v/v) fetal calf serum (BioConcept, Allschwil, Switzerland). Subcultures were obtained twice a week from confluent cell monolayers using a split

ratio of 1:4. Human astrocytoma 1321N1 cells were cultured in the presence of 0.25 mg/mL geneticin to maintain P2X receptor expression levels.

HEK-hP2X7 cell line overexpressing P2X7

HEK293 cells (HEK-hP2X7) were generated according to established molecular cloning protocols. Specifically, RNA was extracted from human whole blood using the Qiagen RNeasy kit (Qiagen, Hombrechtikon, Switzerland) according to the manufacturer's instructions. Subsequently, cDNA was generated (Superscript II, Life Technologies), and the human P2X7 gene (gene bank ref. BC011913) was amplified and ligated into a pcDNA3.1 (+) vector. HEK293 cells (CRL 1573, ATCC American type culture collection, Manassas, VA) were transfected with the pcDNA3.1 (+) hP2X7 plasmid using lipofectamine transfection reagent (Life Technologies) according to the manufacturer's instructions. After exposure to DNA for 24 h, cells were trypsinized and reseeded at low density in the presence of 0.25 mg/mL geneticin. Geneticin-resistant cells were then selected in two consecutive rounds of cloning by serial limiting dilution with visual inspection. Individual clones were screened for P2X7 expression by applying ATP and recording the resulting uptake of YoPro1. A specific cell clone was chosen based on RNA and protein expression. Parental HEK293 cells and HEK-hP2X7 cells were cultured under standard cell culture conditions in DMEM with 2.0 mmol/L L-glutamine (Life Technologies) supplemented with 50 IU/mL penicillin, 50 μ g/mL streptomycin, and 10% (v/v) fetal calf serum (BioConcept). Subcultures were obtained twice a week from confluent cell monolayers using a split ratio of 1:5. HEK-hP2X7 cells were cultured in the presence of 0.25 mg/mL geneticin to maintain P2X7-expression levels. Under these conditions, cells expressed constant levels of P2X7 for at least 30 passages.

Mouse microglia BV2 cells

The mouse microglia BV2 cell line used for patch-clamp experiments was cultured under standard cell culture conditions. The cells were maintained in DMEM with 2 mmol/L GlutaMAX (Life Technologies) supplemented with 50 IU/mL penicillin, 50 μ g/mL streptomycin, and 10% (v/v) fetal calf serum (BioConcept).

Electrophysiology

For patch-clamp experiments, mouse microglia BV2 cells were analyzed in the whole-cell patch-clamp configuration (Hamill *et al.* 1981). Several P2X7-mouse models have shown different splice variants of the P2X7-receptor and

therefore a lack of functionality. In-process control experiments showed functionality of the P2X7 receptors in the used BV2 cells (data not shown). Patch electrodes were filled with intracellular buffer containing 120 mmol/L KF, 20 mmol/L KCl, 1.0 mmol/L ethylene glycol-bis(aminoethyl ether)-tetraacetic acid (EGTA), and 10 mmol/L 4-(2-hydroxyethyl)-1-piperazineethanesulfonic acid (Hepes) adjusted to pH 7.2 with potassium hydroxide. Recordings were done at room temperature in external buffer containing 147 mmol/L NaCl, 2.0 mmol/L KCl, 0.3 mmol/L CaCl₂, 10 mmol/L Hepes, and 12 mmol/L D-glucose adjusted to pH 7.4 with sodium hydroxide. At a constant holding potential of -70 mV, BzATP (100 μmol/L) was added in the presence or absence of different concentrations of the P2X7-receptor antagonist by a computer-controlled application system. Agonist-induced steady-state currents were corrected for leak, and concentration-response curves were fitted to averaged current amplitudes derived from 3 to 4 cells.

Fluo-4-AM calcium measurements

Intracellular calcium concentrations were determined using human astrocytoma 1321N1 cell overexpressing human P2X1, P2X2, P2X3, P2X4, or P2X7 receptor. Cells were loaded with 4.0 μmol/L Fluo-4-AM in Hank's balanced salt solution (HBSS; Life Technologies) containing 20 mmol/L Hepes, pH 7.4. Cells were washed once at 10 min before recording. After preincubation with 10 μmol/L of AZD9056 for 2 min ATP was added at final concentrations of 0.2–2 mmol/L and signals recorded after 15 min. Fluorescence signals were measured using a fluorescent imaging plate reader.

YoPro1 uptake analysis

The membrane-impermeable fluorescent dye YoPro1 was used to determine P2X7-receptor permeability for larger ions (Rassendren et al. 1997; Michel et al. 1998). HEK-hP2X7 cells were diluted in cell culture medium without geneticin to a final concentration of 2×10^5 cells/mL, and an aliquot (50 μL) of this cell suspension was transferred to a poly-L-lysine precoated black-wall, clear-bottom plate and incubated at 37°C in a humidified atmosphere containing 5% CO₂ for 48 h. The medium was then removed from cells, and assay buffer containing 0.5 μmol/L YoPro1 was added to the wells. Cells were incubated with the indicated concentrations of AZD9056 and ATP at a final concentration of 250 μmol/L for 45 min. Fluorescence signals were measured using a fluorescent imaging plate reader (tetra, Molecular Device, Sunnyvale, CA). Excitation wavelength and emission wavelength were 485 and 530 nm, respectively.

Hydrogen peroxide generation by mononuclear cells

Production of cellular H₂O₂ by mononuclear blood cells after stimulation with P2X7 agonists (ATP or BzATP) was determined by the Amplex Red assay (Life Technologies). Briefly, 5×10^5 mononuclear blood cells were incubated with 50 μmol/L Amplex Red and 0.1 U/mL horseradish peroxidase for 0.5 h at 37°C in Krebs Ringer phosphate solution (145 mmol/L NaCl, 5.7 mmol/L sodium phosphate, 4.9 mmol/L KCl, 0.5 mmol/L CaCl₂, 1.2 mmol/L MgSO₄, and 5.5 mmol/L glucose) protected from light. After adding ATP (1 mmol/L) or BzATP (0–400 μmol/L) to the cells, the fluorescence was quantified by means of a microplate reader (Synergy MX, BioTek®, Luzern, Switzerland) at an excitation wavelength of 550 nm and absorbance wavelength of 600 nm. Background fluorescence was determined in a reaction without mononuclear blood cells.

Cytosensor experiments

HEK-hP2X7 cells and parental HEK293 cells were detached by trypsinization (Life Technologies), and cell viability was analyzed. Cells were then diluted in culture medium to a final concentration of 5.7×10^5 cells/mL. An aliquot (0.35 mL) of this cell suspension was transferred to the pre-warmed fibronectin-coated sensor chip (SC1000) and incubated for at least 20 h prior to use. A cytosensor system (Bionas 1500 system, Bionas, Rostock, Germany) was used to continuously record cellular physiology parameters as described previously (Seeland et al. 2011). Briefly, a flow head with 50 μm spacers (as determined by the distance between the flow head and sensor chip surface) was used, leading to an effective chamber volume of 1.4 μL. The assay medium used was DMEM supplemented with 2.0 mmol/L L-glutamine, 0.1% (v/v) fetal bovine serum, 25 IU/mL penicillin, and 25 μg/mL streptomycin. The assay medium contained neither Hepes nor NaHCO₃ and was adjusted to pH 7.4 using sodium hydroxide. During analysis, the assay medium was delivered to the cells at a constant flow rate (63 μL/min) and interrupted periodically (stop phases of 4 min and pump phases of 3 min). Signals from the microsensor chip were recorded after a stabilization phase of at least 3 h. During three stop/go cycles (21 min in total), cells were exposed to increasing concentrations of the agonist BzATP (0–100 μmol/L) in assay medium and adjusted to pH 7.4 using sodium hydroxide. In experiments with BzATP, cells were exposed to AZD9056 (10 μmol/L) prior to treatment with 50 μmol/L BzATP. Stimulation and/or inhibition phases with BzATP and/or AZD9056 were followed by a wash-out phase of at least 4 h before a new stimulation phase was initiated.

Cellular viability assay

The effect of agonists on cell viability was assessed in parental HEK293 cells and HEK-hP2X7 cells using the CellTiter-Blue assay according to the manufacturer's instructions. In brief, an aliquot (60 μ L) of cell suspension with a nominal cell density of 8×10^6 cells/mL was dispensed into a 96-well plate. The cells were incubated for 24 h in a humidified atmosphere containing 5% CO₂ to allow cell attachment. At the end of the preincubation period, ATP or BzATP was added to the cells at concentration ranges up to 5 mmol/L and 0.5 mmol/L, respectively. For inhibition experiments, AZD9056 was added to the cells at concentrations up to 10 μ mol/L 5 min prior to the addition of ATP (2.5 mmol/L) or BzATP (0.25 mmol/L). After incubation for 30 min at 37°C, an aliquot (20 μ L) of the prewarmed CellTiter-Blue reagent was added. Samples were incubated for 1 h at 37°C. Fluorescence signals were measured using a fluorescent imaging plate reader (tetra, Molecular Device). Excitation and emission wavelengths were 560 and 590 nm, respectively.

Mitochondrial membrane potential

To determine mitochondrial membrane potential ($\Delta\psi/m$), JC-1 cyanine dye was used as a marker for mitochondrial integrity. In cells with intact membrane potential, JC-1 dye forms orange aggregates within the mitochondria. Depolarization of the mitochondrial membrane leads to JC-1 disaggregation and a shift of the fluorescence emission wavelength. Parental HEK293 cells and HEK-hP2X7 cells were seeded on a poly-D-lysine-coated Ibidi μ -Slide (Vitaris AG, Baar, Switzerland) to reach a final cell density of 5×10^4 cells per well. Cells were allowed to adhere overnight. Then, JC-1 dye was added to the medium at a final concentration of 10 μ g/mL. Cells were incubated for 15 min at 37°C allowing the dye to accumulate within the mitochondria. Subsequently, the medium was removed, and cells were carefully rinsed with prewarmed PBS and incubated for 1 h at 37°C with medium containing BzATP at concentrations of 31.3 or 250 μ mol/L. The K⁺ ionophore valinomycin (1 mmol/L) served as a positive control, while untreated cells were used as a negative control. Fluorescence emission was monitored with an IX81 Olympus confocal microscope at 37°C in an atmosphere containing 5% CO₂. JC-1 aggregates were excited with a laser at 559 nm, and emission was recorded with a wavelength filter in the range of 574–627 nm. JC-1 monomers were excited at 488 nm, and emission was recorded with a wavelength filter in the range of 500–535 nm as described earlier (Perelman et al. 2012).

Data analysis and statistics

Concentration–response curves were obtained from experiments with the cell-based microsensor system in the presence or absence of the antagonist. Evaluation as well as kinetic and statistic calculations were performed using GraphPad Prism software (Version 5.04; GraphPad Software Inc., La Jolla, CA). Results were expressed as means of at least three independent experiments \pm SD or means with 95% confidence intervals (CI). Statistical differences were determined by Student's *t*-test.

Results

Electrophysiology of P2X7-receptor activation and effects on calcium and YoPro1 dye influx

Figure 1A shows the activation of the P2X7 receptor by BzATP as studied in patch-clamp experiments using the P2X7 receptor-expressing mouse microglia BV2 cell line. Effects were characterized by an EC₅₀ of 197 ± 5.1 μ mol/L (mean \pm SD, $n = 5$). The P2X7-receptor antagonist AZD9056 inhibited BzATP-induced currents in these cells (Fig. 1B). BzATP induced stable, inward currents at a holding potential of -70 mV that were blocked by AZD9056 with an IC₅₀ of 1–3 μ mol/L (95% CI, 1.8–2.5 μ mol/L, $n \geq 5$; Fig. 1C).

Selectivity of AZD9056 toward P2X7

Remaining receptor activity by monitoring Ca²⁺ influx into human astrocytoma 1321N1 cells overexpressing P2X1, P2X2, P2X3, P2X4, or P2X7 was performed to assess the selectivity of AZD9056 toward P2X7 (Fig. 1D). Subsequently, 1321N1 cells were activated for 15 min by the addition of ATP. The addition of 10 μ mol/L AZD9056 showed no effect in activity on P2X1–3. A decrease of 27% in the remaining activity was observed in 1321N1 cells expressing P2X4 receptors, whereas cell expressing P2X7 receptors exhibited a remaining activity of 9%.

YoPro1 influx was determined upon stimulation of HEK-hP2X7 cells with BzATP for 45 min. Observed effects were antagonized with an IC₅₀ of 11.2 nmol/L (95% CI, 9.6–13.2 nmol/L; Fig. 1E).

ATP-induced hydrogen peroxide release by mononuclear blood cells

Mononuclear cells were freshly prepared from human donor blood. Within 20 min, exogenously applied ATP induced a marked, concentration-dependent increase in H₂O₂ release with an EC₅₀ of 558 ± 8.7 μ mol/L

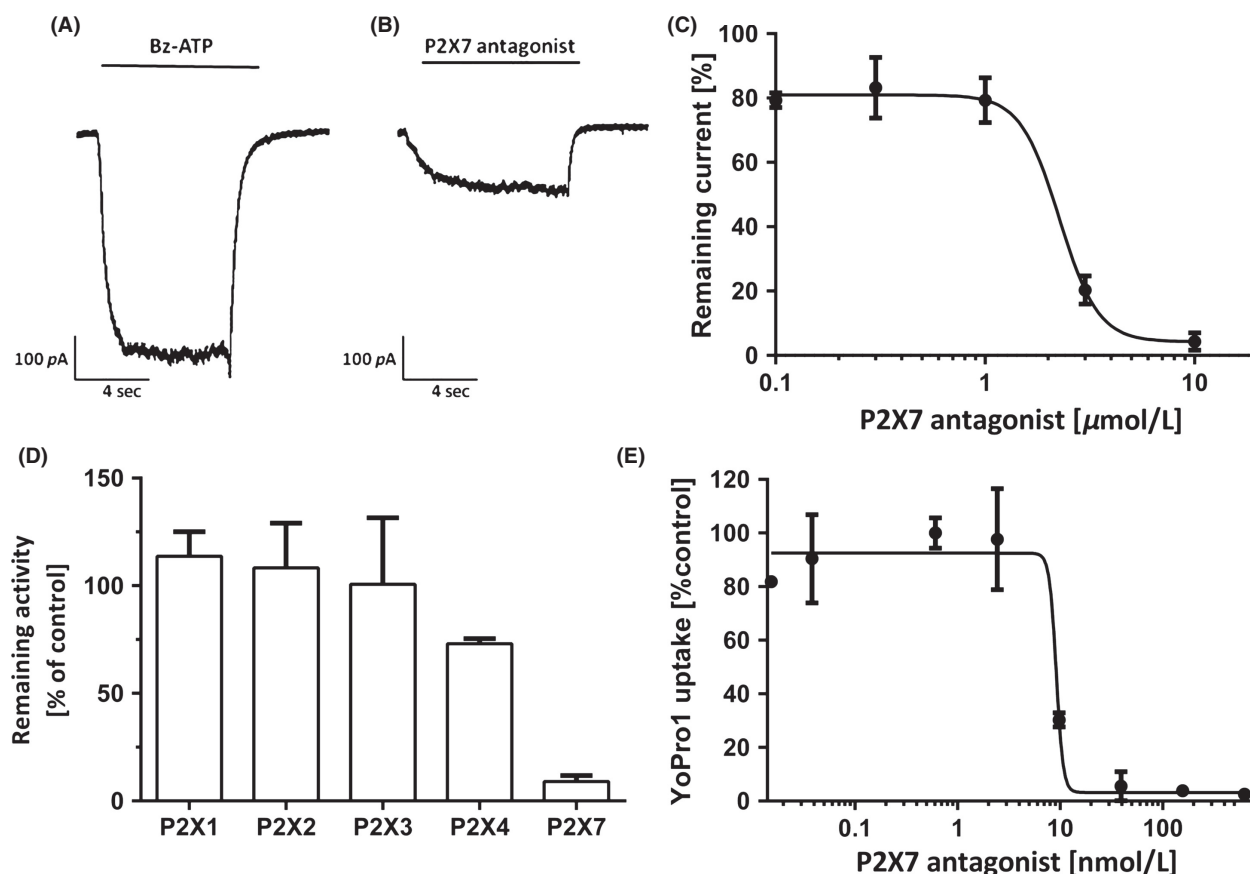


Figure 1. Patch-clamp experiments using P2X7-receptor-expressing mouse microglia BV2 cells. (A) Raw current signal pattern after stimulation of BV2 cells using 100 $\mu\text{mol/L}$ BzATP. (B) Raw current signal pattern after stimulation of BV2 cells using 100 $\mu\text{mol/L}$ BzATP in the presence of 10 $\mu\text{mol/L}$ of AZD9056. (C) Dose-dependent inhibition of membrane currents in mouse microglia BV2 cells using AZD9056. Cells were stimulated using 100 $\mu\text{mol/L}$ BzATP. (D) Remaining receptor activity in human astrocytoma 1321N1 cells overexpressing human P2X1, P2X2, P2X3, P2X4, or P2X7 receptor monitored by Ca^{2+} flux upon activation with ATP and inhibition with 10 $\mu\text{mol/L}$ AZD9056. (E) YoPro1 dye membrane permeability measurements using P2X7-overexpressing HEK-hP2X7 cells stimulated by 250 $\mu\text{mol/L}$ ATP in the presence of increasing concentrations of AZD9056. (C, D, E). Values are means \pm SD, $n \geq 4$.

(mean \pm SD, $n = 3$), as depicted in Figure 2A. The P2X7-specific receptor antagonist AZD9056 elicited moderate inhibition of H_2O_2 formation with an IC_{50} of $3.0 \pm 0.9 \mu\text{mol/L}$ (mean \pm SD, $n = 3$) at 1 mmol/L ATP, indicating involvement of the P2X7 receptor (Fig. 2B).

BzATP-induced metabolic activation of HEK239 cells and HEK-hP2X7 cells overexpressing P2X7

We used a cytosensor system for real-time monitoring of metabolic activation of HEK-hP2X7 cells. Measured parameters were oxygen concentration, pH, and cell impedance. The sensor system was optimized with respect to maximum stimulation amplitudes, as described previously (Seeland et al. 2011). Optimal cell density was

2×10^5 attached cells per sensor chip and an effective incubation chamber volume of 1.4 μL . Viability of cells was monitored continuously by measuring cellular impedance. Continuous deviations from initial values in the order of approx. $\pm 1.2\%$ per hour were considered acceptable and were attributed to cell proliferation or cell release from the chip. HEK-hP2X7 cells responded immediately to BzATP in a concentration-dependent manner (Fig. 3). In HEK-hP2X7 cells but not in HEK293 control cells, metabolic activity (i.e., acidification) and cellular respiration increased in a concentration-dependent manner upon BzATP treatment (Fig. 3A). At high BzATP concentrations (100 $\mu\text{mol/L}$), a sharp decrease in cellular respiration was observed, which was in strict contrast to cellular acidification. The respiration collapse at the highest concentration of agonist is indicative for cellular toxicity. The resulting impairment in the generation of ATP

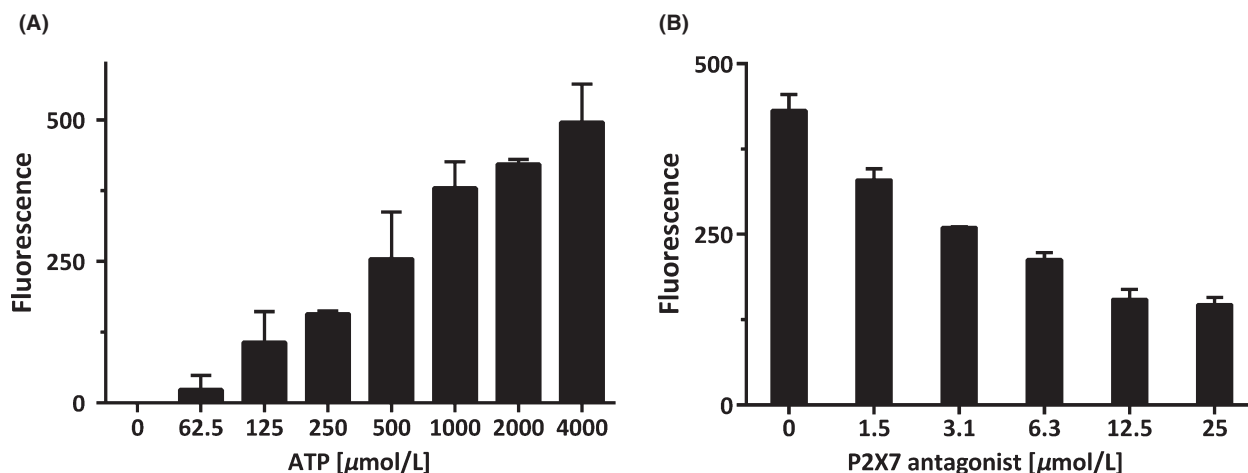


Figure 2. P2X7-mediated cellular formation of hydrogen peroxide. (A) Rate of H₂O₂ formation in mononuclear blood cells after stimulation with extracellular ATP. (B) Effect of the P2X7 antagonist AZD9056 on H₂O₂ levels in mononuclear blood cells stimulated with 1 mmol/L ATP. Values are means \pm SD, $n = 6$ measurements.

via oxidative phosphorylation is compensated to a certain extent by the enhancement in metabolic activity, monitored by an increase in extracellular acidification. At very high agonist concentrations, these compensatory mechanisms will eventually fail leading to a respiratory collapse. Maximum changes in cell morphology (i.e., impedance) were reached at 100 μ mol/L BzATP (Fig. 3B). Compared to HEK-hP2X7 cells, parental HEK293 cells showed only negligible effects on the impedance sensor (Fig. 3B).

Activation of the P2X7 receptor by BzATP was saturated at high concentrations and was characterized by an EC₅₀ of 9.6 ± 1.8 μ mol/L (mean \pm SD, $n = 5$; Fig. 3B). Activation of P2X7 receptor was therefore assessed using agonist concentration of 10 μ mol/L (Fig. 4). This concentration is close to the system-dependent EC₅₀ of 9.6 μ mol/L and can therefore be used to target statistical significant effects. In addition, potential saturation or interference with biological functions in the target cells can be avoided. These effects were inhibited by AZD9056 (Fig. 4). Inhibitory effects of AZD9056 were reversible since responsiveness of the cells toward BzATP was partially restored by washing out the antagonist (Fig. 4). Inhibition of the BzATP-induced effects observed in HEK-hP2X7 cells overexpressing P2X7 did not take place in the parental HEK293 cells (Fig. 4).

ATP- and BzATP-induced cytotoxicity

Stimulation of P2X7-expressing HEK-hP2X7 cells with ATP (Fig. 5A) or BzATP (Fig. 5B) resulted in concentration-dependent cytotoxic effects. These effects were absent in parental HEK293 cells. LD₅₀ values for HEK-hP2X7 cells were 1017 ± 81 μ mol/L (mean \pm SD, $n = 3$) for

ATP and 119.7 ± 4.4 μ mol/L (mean \pm SD, $n = 3$) for BzATP. These effects were antagonized by AZD9056 with an IC₅₀ of 11.4 ± 1.8 nmol/L (mean \pm SD, $n = 3$) at 2.5 mmol/L ATP (Fig. 5C) and 5.62 ± 0.75 nmol/L (mean \pm SD, $n = 3$) at 0.25 mmol/L BzATP (Fig. 5D). Again, parental HEK293 cells were not responsive to ATP, BzATP, or AZD9056 (Fig. 5C and D).

BzATP-induced mitochondrial toxicity

Figure 6 shows a decrease of mitochondrial membrane potential ($\Delta\psi_m$) in BzATP-treated HEK-hP2X7 cells (but not in P2X7-deficient control cells) as visualized by a change from red to green fluorescent signals in the target cells. The shift in the emission spectrum of the cyanine dye JC-1 was monitored upon stimulation of HEK-hP2X7 cells for 1 h with elevated concentrations of BzATP (30–250 μ mol/L). Valinomycin, a K⁺ ionophore, served as a positive control.

Discussion

This study investigated the effect of the P2X7-receptor agonists ATP and the metabolically stable analogue BzATP (Le Feuvre et al. 2003) on different P2X7-expressing cell lines. ATP as well as BzATP are not selective P2X7 receptor agonists. Both stimulate all P2X receptors at low concentrations. In vitro concentrations of ATP needed to reach equal stimulatory effects as BzATP are at least 10-fold greater than that of BzATP. This can be attributed to the low chemical stability of ATP, which makes an assessment of actual concentrations of the agonist at its site of action difficult. Real-time monitoring

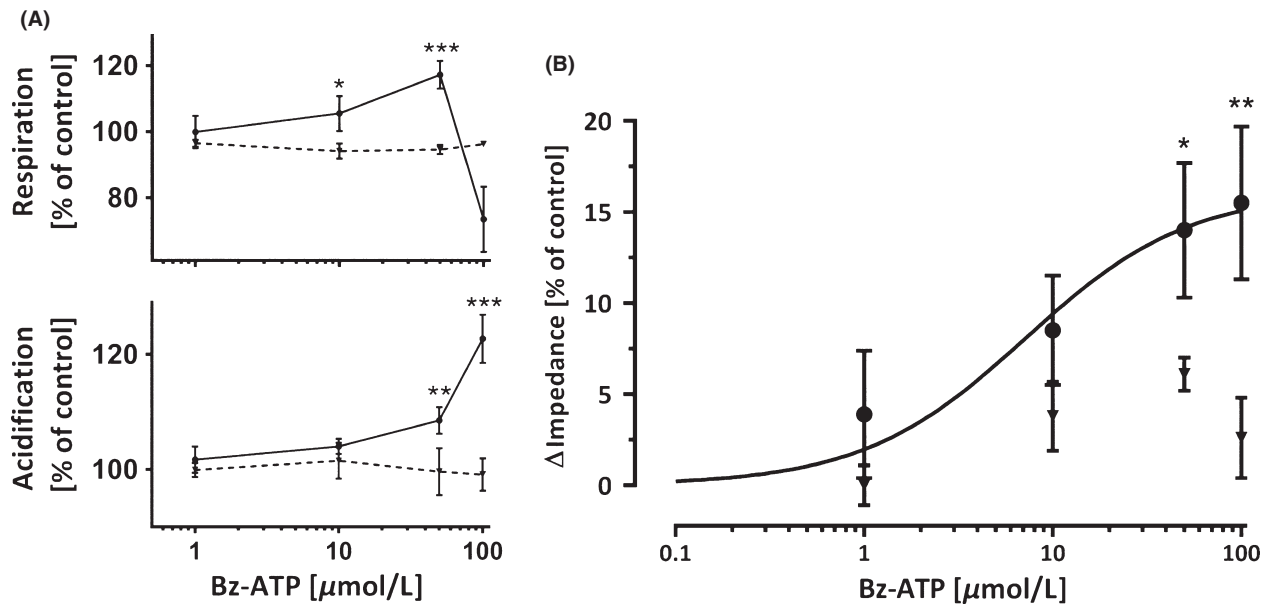


Figure 3. Cytosensor measurements in HEK-hP2X7 cells overexpressing P2X7 and parental HEK293 cells. (A) Concentration-dependent stimulation of HEK-hP2X7 cells (solid lines, black circles) and parental HEK293 cells (dotted lines, inverted triangles) by BzATP as analyzed using a cytosensor system. Parental HEK293 cells and human HEK-hP2X7 cells were compared with respect to respiration and metabolic activity (acidification). Respiratory inhibition in HEK-hP2X7 cells at 100 $\mu\text{mol/L}$ BzATP was indicative of cellular toxicity. Level of significance: * $P < 0.05$, ** $P < 0.01$, *** $P < 0.001$, $n = 4$. (B) Cell impedance as a function of stimulation of P2X7 using BzATP. Curve was fitted to HEK-hP2X7 signals (solid line, black circles) using an enzyme kinetic model. Parental HEK293 cells were used as a control (inverted triangles). Level of significance: * $P < 0.05$, ** $P < 0.01$, $n = 4$.

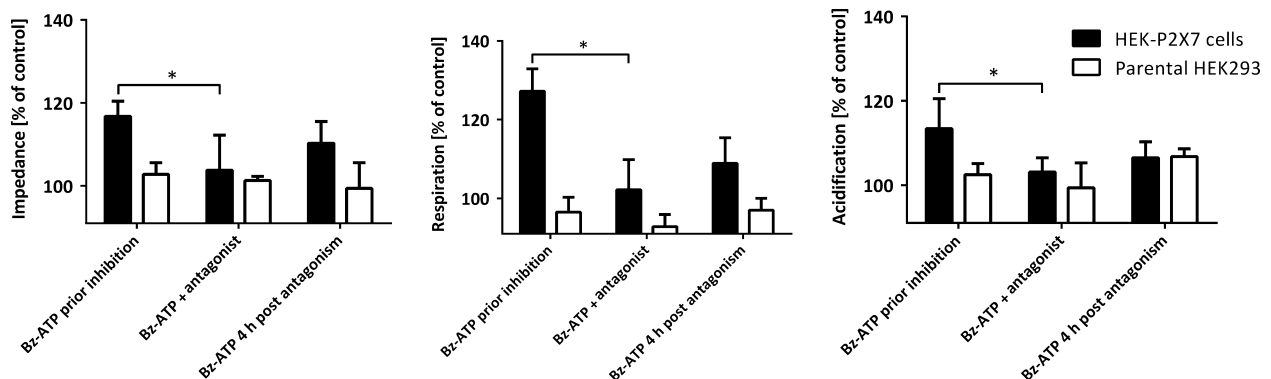


Figure 4. Reversible inhibition of BzATP-induced effects by AZD9056. Cytosensor measurements using HEK-hP2X7 cells and parental HEK293 cells in the presence and absence of 10 $\mu\text{mol/L}$ AZD9056. After a wash-out period of 4 h, the cells were again stimulated with 50 $\mu\text{mol/L}$ BzATP to assess regeneration and reactivation. Level of significance in the presence and absence of antagonist: * $P < 0.05$, $n = 4$.

of the effects for the timescale of seconds was achieved electrophysiologically and for the timescales up to minutes and hours using a novel cytosensor system. The real-time cytosensor system is able to monitor stimulation and antagonistic effects on the P2X7 receptor in ranges from seconds, minutes and up to several hours. Compared to the very fast electrophysiological assays (milliseconds) and the slow biochemical assays (hours), the cytosensor covers

an intermediate time window, which is not accessible in the alternative assays. With this respect, the cytosensor allows simultaneous monitoring of toxicological effects on mitochondrial respiration and energy metabolism on a cellular level, as well as cell morphological changes upon agonist stimulation (Seeland et al. 2013). We propose to use a combination of the assays used in this study to monitor the entire process of P2X7 activation from the millisecond

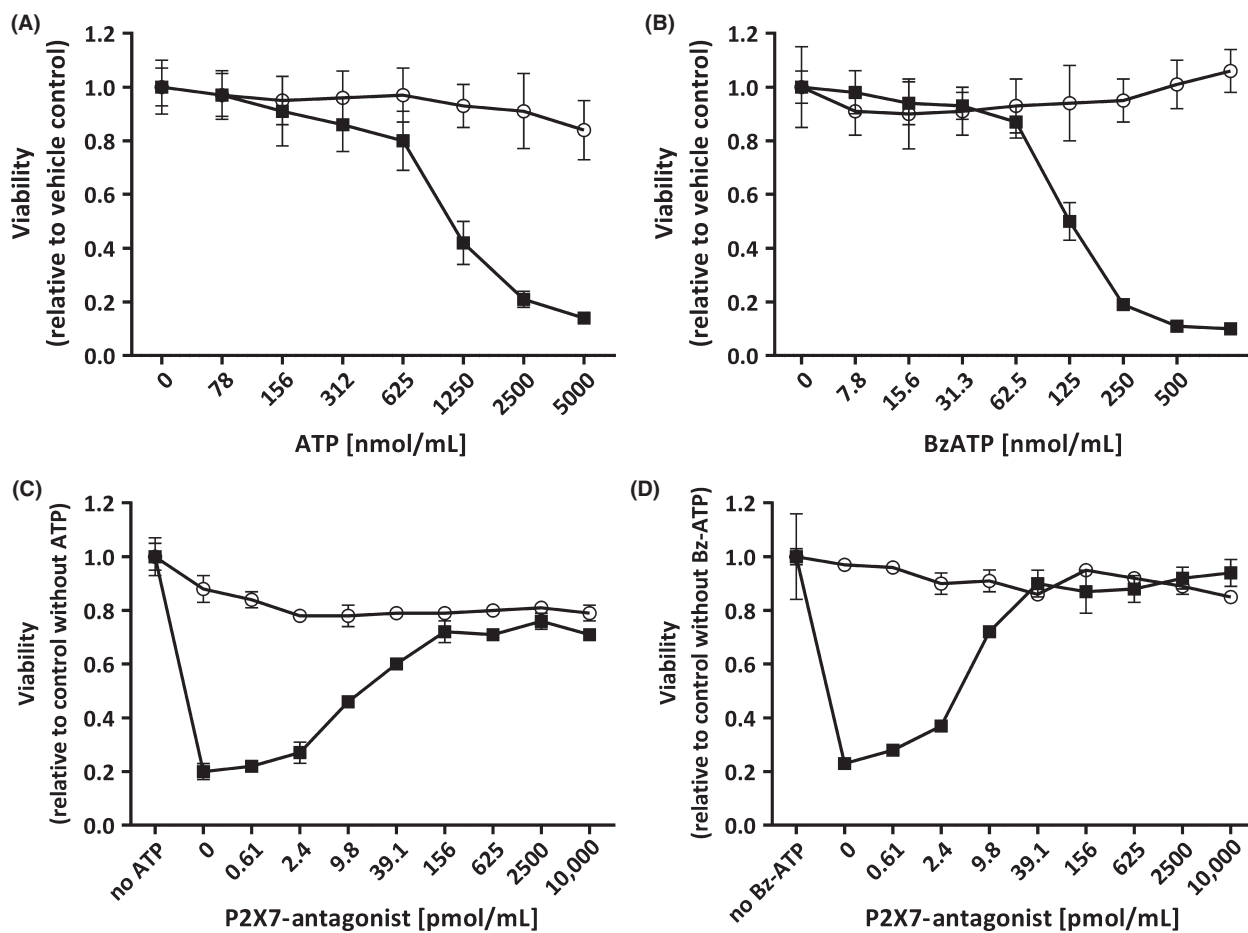


Figure 5. Cellular viability of parental HEK293 cells (empty circles) and HEK-hP2X7 cells (filled squares). Cellular viability was analyzed in the presence of increasing concentrations of the two P2X7 agonists (A: ATP; B: BzATP). A cell-protective function of the P2X7-specific antagonist AZD9056 was demonstrated in inhibition experiments where cells were preincubated with increasing concentrations of a P2X7-specific antagonist (AZD9056) prior to addition of the agonists ATP (C: 2.5 mmol/L) or BzATP (D: 0.25 mmol/L). Values presented as means \pm SD, $n = 5$ measurements.

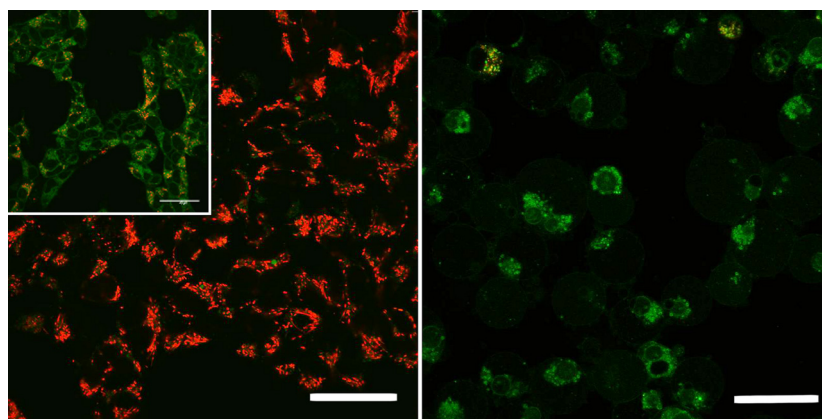


Figure 6. Induction of mitochondrial toxicity in HEK-hP2X7 cells. Parental HEK293 (left panel) and HEK-hP2X7 (right panel) cells were stimulated using 250 μ mol/L BzATP. A decrease in mitochondrial membrane potential is indicated by a shift from red fluorescent signals to green fluorescent signals. Insert, left panel: 1 mmol/L valinomycin was used as a positive control. Size of bars: 40 μ m.

to the hours range. The effects were highly specific for P2X7 as demonstrated by the use of P2X7-deficient control cells and the selective P2X7-receptor antagonist AZD9056 (Bhattacharya et al. 2011; Elsby et al. 2011). Activation of P2X7 had a direct impact on membrane permeability for ions, intracellular calcium release, cell morphology (i.e., swelling), and cellular respiration and metabolism (Table 1). This induced oxidative and metabolic stress in target cells, ultimately leading to cellular toxicity and cell death. The assays used in the study have different optimum EC_{50} values and therefore the agonist concentrations are adapted to gain an assay-specific optimized readout. A drawback of this approach is that the antagonist concentration cannot directly be compared, thus differences in assay conditions (e.g., buffer compositions, agonist concentrations, assay conditions) lead to the wide range of apparent antagonist potencies reported in Table 1.

In order to characterize the human P2X7 receptor, a recombinant HEK-hP2X7 cell line was prepared. Functionality of the recombinant human P2X7 receptor was confirmed using the YoPro1 uptake assay upon stimulation of the target cells with ATP. The antagonist AZD9056 blocked P2X7 receptors with an IC_{50} of 11.2 nmol/L, indicating a high selectivity of the antagonist for the P2X7 receptor. This IC_{50} value is comparable to values determined previously for mouse and rat P2X7 receptors (in the order of 1–2 nmol/L, data not shown). Thus, the YoPro1 uptake experiment allowed comparing and confirming the pharmacological properties of the P2X7 receptor in our study with those determined with methods traditionally used for studying the P2X7 receptor. Furthermore, the characteristics of human P2X7 receptor in this cell line were similar to those of rodent P2X7 receptor expressed by mouse microglia BV2 cells, as demonstrated electrophysiologically. In these experiments, patch-clamp techniques were used to measure directly the flux of small, inorganic ions across the P2X7 channels.

Mouse microglia BV2 cells express both P2X7 and P2X4 receptors (Bernier et al. 2012). BzATP showed effects on receptor activity, and the P2X7-receptor antagonist AZD9056 had a clear inhibitory effect ($IC_{50} = 1–3 \mu\text{mol/L}$), which allows to attribute the effects to the P2X7 receptor.

It is not possible to deduce a clear pathway from ATP-gated channel opening to the activation of cellular metabolism. However, small cations (e.g., Ca^{2+}) as well as larger molecules entering the cell upon P2X7-receptor pore opening are known to trigger further downstream effects such as interleukin- 1β release, MAPK activation, apoptosis, etc., and are therefore linked to cell signaling and cell death (Kukley et al. 2005; Ferrari et al. 2006). Hydrogen peroxide (H_2O_2), a metabolic side product of cell respiration, can be used as a marker for cellular toxicity (Giorgio et al. 2007). We measured H_2O_2 released in human mononuclear blood cells upon ATP treatment and found that ATP induced a concentration-dependent increase in H_2O_2 release, confirming previous reports (Skaper et al. 2006). It should be noted that the concentration–response curve for ATP induction of H_2O_2 release with an EC_{50} above 0.5 mmol/L did not fit with the ATP sensitivity of the 12 known metabotropic P2Y receptors. Only the P2X7 receptor exhibits such low sensitivity to extracellular ATP (Coddou et al. 2011). Our hypothesis was supported by experiments with the antagonist AZD9056 that achieved concentration-dependent inhibition of ATP-induced H_2O_2 release in human mononuclear blood cells. Furthermore, AZD9056 (10 $\mu\text{mol/L}$) showed no significant inhibition of signaling on P2 receptors in recombinant 1321N1 cells overexpressing P2X1, P2X2, P2X3, and P2X4 when measuring Ca^{2+} flux after ATP stimulation. In contrast, remaining receptor activity in 1321N1 cells overexpressing P2X7 exhibits a significant decrease in P2X7 activity upon treatment with the antagonist AZD9056. AZD9056 can therefore be considered to be selective for the P2X7 receptor, in contrast to other

Table 1. Summary of agonist-induced and antagonist-induced effects mediated by the P2X7 receptor.

Assay	Cells	Agonist ¹ [$\mu\text{mol/L}$]	P2X7-receptor antagonist ² [$\mu\text{mol/L}$]	IC_{50} or % inhibition
Patch-clamp	Mouse microglia	100	0.3–10	1–3 $\mu\text{mol/L}$ 96% ³
Peroxide release	Mononuclear blood cells	1000	0–25	3.0 $\mu\text{mol/L}$
YoPro1 uptake	HEK-hP2X7	3000	3.8×10^{-5} –10	11.2 nmol/L
Sensor system respiration	HEK-hP2X7	50	10	92%
Sensor system acidification	HEK-hP2X7	50	10	77%
Sensor system impedance	HEK-hP2X7	50	10	77%

¹Assays for H_2O_2 release and YoPro1 uptake were performed with ATP, all other assays with BzATP.

²P2X7-receptor antagonist AZD9056.

³At 10 $\mu\text{mol/L}$ AZD9056.

known antagonists of P2 receptors such as suramin and pyridoxal-phosphate-6-azophenyl-2',4'-disulphonic acid (PPADS) (Chessell *et al.* 1998; Ralevic and Burnstock 1998). The concentration of BzATP used was one tenth (400 $\mu\text{mol/L}$) of the concentration of ATP (4000 $\mu\text{mol/L}$) and induced equal H_2O_2 release from human mononuclear blood cells at these concentrations indicating the potent effects of BzATP toward P2X7. BzATP was chosen for these experiments since it is a stable ATP analogue for both P2X4 and P2X7 receptors with only partial activity toward P2X1, P2X2, and P2X3 receptors (Coddou *et al.* 2011).

We subsequently used the HEK-hP2X7 cells overexpressing P2X7 to study changes in metabolic activity in real time by means of a cell-based cytosensor system. We were able to record simultaneously extracellular acidification as a marker for metabolic activity, oxygen consumption as a measure for cellular respiration, and impedance as a means to assess changes in cell morphology and adhesion. P2X7 receptors are colocalized with α -actin, β -actin, and the β 2-integrin subunit, that is, factors that determine changes in the cytoskeleton (Kim *et al.* 2001). Pfeiffer *et al.* (2004) previously described morphological changes in cells expressing P2X7 receptors when P2X7 agonists were present. We confirmed these morphological changes by measuring cellular impedance. Morphological changes upon ATP treatment are an indication of ligand binding to the human P2X7 receptor (Pfeiffer *et al.* 2004) and can therefore be used to calculate EC_{50} values of activation. In addition, HEK-hP2X7 cells exhibited concentration-dependent swelling upon treatment with BzATP, possibly reflecting the osmotic influx of water into the cells due to pore dilatation. We estimated the potency of BzATP to induced morphological changes using an enzyme kinetic model ($\text{EC}_{50} = 9.6 \mu\text{mol/L}$). Cellular respiration was maximally increased at 50 $\mu\text{mol/L}$ BzATP when compared with parental cells. Treatment with 100 $\mu\text{mol/L}$ BzATP, however, led to a sharp drop in respiration, which indicates mitochondrial toxicity (Gandelman *et al.* 2010). The resulting impairment in the generation of ATP via oxidative phosphorylation was compensated to a certain extent by the enhancement in metabolic activity, monitored by an increase in extracellular acidification. Strong amplification of metabolic activity under these conditions (monitored by an increase in extracellular acidification) clearly indicates a compensatory cellular response in terms of enhanced glycolysis. Reduction in cellular respiration was probably linked to both the formation of reactive oxygen species (Skaper *et al.* 2006) and activation of the apoptosis cascade (Hillman *et al.* 2003). The distinctness of stimulatory effects observed in the cytosensor system confirms that the effects mostly derived from the highly expressed P2X7

receptors rather than from other endogenously expressed P2 receptors in HEK293 cells. These results are in line with our findings for H_2O_2 formation by mononuclear cells. Using the cytosensor system, we were able to determine simultaneously multiple variables of cellular metabolism, thus providing a more complete picture of how ATP affects cellular metabolism via the P2X7 receptor. All effects on cell morphology, mitochondrial respiration, and metabolic activity were induced at 50 $\mu\text{mol/L}$ BzATP and were inhibited with 10 $\mu\text{mol/L}$ AZD9056 at potencies between 77% and 92%. Because parental HEK293 cells did not respond to activation or inhibition, all effects observed in HEK-hP2X7 cells appear to be mediated by the human P2X7 receptor.

Prolonged stimulation of HEK-hP2X7 cells with ATP or BzATP led to cytotoxicity. This effect was also dose-dependent, was antagonised by AZD9056, and was not observed in P2X7-deficient HEK293 control cells. Our mechanistic studies revealed a collapse of mitochondrial membrane potential and mitochondrial integrity under these conditions. These findings are in line with our results from cytosensor studies and confirm that mitochondrial toxicity is indeed a trigger for P2X7-mediated cytotoxicity.

We conclude that an increase in membrane leakiness led to disturbance of mitochondrial membrane potential, mitochondrial toxicity, and oxidative stress. Metabolic activity by glycolysis increased as a compensatory mechanism due to the lack of energy generated by oxidative phosphorylation. Prolonged stimulation led to morphological changes and cytotoxicity. Further experiments are necessary to investigate the specificity of these effects and to clarify their role under normal or pathological conditions. Extracellular ATP has been shown to be a key player in triggering inflammatory processes, cellular stress, and apoptosis. Our investigations demonstrate that these processes are tightly linked to oxidative and metabolic activity, which we were able to monitor in real-time simultaneously with an additional confirmation of agonist-induced changes in cell morphology.

Acknowledgements

We thank Kyle Landskroner and Johannes Mosbacher for helpful discussions, Silvia Rogers for editorial assistance, and Michael Nicollier for technical support.

Author Contributions

S. Seeland participated in research design, data interpretation, and performed the cytosensor experiments. M. Murphy and J. Giller prepared the HEK-hP2X7 cell line and performed the hydrogen peroxide release assay. H. Kettiger

did the cytotoxicity experiments. R. Sube and A. Kiss performed the electrophysiology and Ca^{2+} -uptake experiments, respectively. A. Treiber, S. Krähenbühl, and M. Hafner helped essentially with interpretation of data and proposed further steps in the research study. J. Huwyler designed the research study and helped with interpretation of data.

Disclosures

None declared.

References

- Arbeloa J, Perez-Samartin A, Gottlieb M, Matute C (2012). P2X7 receptor blockade prevents ATP excitotoxicity in neurons and reduces brain damage after ischemia. *Neurobiol Dis* 45: 954–961.
- Armstrong JN, Brust TB, Lewis RG, MacVicar BA (2002). Activation of presynaptic P2X7-like receptors depresses mossy fiber-CA3 synaptic transmission through p38 mitogen-activated protein kinase. *J Neurosci* 22: 5938–5945.
- Bardoni R, Goldstein PA, Lee CJ, Gu JG, MacDermott AB (1997). ATP P2X receptors mediate fast synaptic transmission in the dorsal horn of the rat spinal cord. *J Neurosci* 17: 5297–5304.
- Beaucage KL, Xiao A, Pollmann SI, Grol MW, Beach RJ, Holdsworth DW, Sims SM, Darling MR, Dixon SJ (2013). Loss of P2X7 nucleotide receptor function leads to abnormal fat distribution in mice. *Purinergic Signal* 10: 291–304.
- Beis I, Newsholme EA (1975). The contents of adenine nucleotides, phosphagens and some glycolytic intermediates in resting muscles from vertebrates and invertebrates. *Biochem J* 152: 23–32.
- Bernier LP, Ase AR, Boue-Grabot E, Seguela P (2012). P2X4 receptor channels form large noncytolytic pores in resting and activated microglia. *Glia* 60: 728–737.
- Bhattacharya A, Neff RA, Wickenden AD (2011). The physiology, pharmacology and future of P2X7 as an analgesic drug target: hype or promise? *Curr Pharm Biotechnol* 12: 1698–1706.
- Billingsley KG, Stern LE, Lowy AM, Kahlenberg MS, Thomas CR Jr (2004). Uncommon anal neoplasms. *Surg Oncol Clin N Am* 13: 375–388.
- Birch RE, Schwiebert EM, Peppiatt-Wildman CM, Wildman SS (2013). Emerging key roles for P2X receptors in the kidney. *Front Physiol* 4: 262.
- Buisman HP, Steinberg TH, Fischbarg J, Silverstein SC, Vogelzang SA, Ince C, et al. (1988). Extracellular ATP induces a large nonselective conductance in macrophage plasma membranes. *Proc Natl Acad Sci USA* 85: 7988–7992.
- Burnstock G (2006). Historical review: ATP as a neurotransmitter. *Trends Pharmacol Sci* 27: 166–176.
- Chessell IP, Michel AD, Humphrey PP (1998). Effects of antagonists at the human recombinant P2X7 receptor. *Br J Pharmacol* 124: 1314–1320.
- Chrovian CC, Rech JC, Bhattacharya A, Letavic MA (2014). P2X7 antagonists as potential therapeutic agents for the treatment of CNS disorders. *Prog Med Chem* 53: 65–100.
- Coddou C, Yan Z, Obsil T, Huidobro-Toro JP, Stojilkovic SS (2011). Activation and regulation of purinergic P2X receptor channels. *Pharmacol Rev* 63: 641–683.
- Cosentino S, Banfi C, Burbiel JC, Luo H, Tremoli E, Abbracchio MP (2011). Cardiomyocyte death induced by ischemic/hypoxic stress is differentially affected by distinct purinergic P2 receptors. *J Cell Mol Med* 16: 1074–1084.
- Dawicki DD, Chatterjee D, Wyche J, Rounds S (1997). Extracellular ATP and adenosine cause apoptosis of pulmonary artery endothelial cells. *Am J Physiol* 273: L485–L494.
- Donnelly-Roberts DL, Namovic MT, Han P, Jarvis MF (2009). Mammalian P2X7 receptor pharmacology: comparison of recombinant mouse, rat and human P2X7 receptors. *Br J Pharmacol* 157: 1203–1214.
- Elsby R, Fox L, Stresser D, Layton M, Butters C, Sharma P, et al. (2011). In vitro risk assessment of AZD9056 perpetrating a transporter-mediated drug-drug interaction with methotrexate. *Eur J Pharm Sci* 43: 41–49.
- Ferrari D, Chiozzi P, Falzoni S, Dal Susino M, Collo G, Buell G, et al. (1997). ATP-mediated cytotoxicity in microglial cells. *Neuropharmacology* 36: 1295–1301.
- Ferrari D, Pizzirani C, Adinolfi E, Lemoli RM, Curti A, Idzko M, et al. (2006). The P2X7 receptor: a key player in IL-1 processing and release. *J Immunol* 176: 3877–3883.
- Gandelman M, Peluffo H, Beckman JS, Cassina P, Barbeito L (2010). Extracellular ATP and the P2X7 receptor in astrocyte-mediated motor neuron death: implications for amyotrophic lateral sclerosis. *J Neuroinflammation* 7: 33.
- Giorgio M, Trinei M, Migliaccio E, Pelicci PG (2007). Hydrogen peroxide: a metabolic by-product or a common mediator of ageing signals? *Nat Rev Mol Cell Biol* 8: 722–728.
- Hamill OP, Marty A, Neher E, Sakmann B, Sigworth FJ (1981). Improved patch-clamp techniques for high-resolution current recording from cells and cell-free membrane patches. *Pflugers Arch* 391: 85–100.
- Hillman KA, Harada H, Chan CM, Townsend-Nicholson A, Moss SE, Miyamoto K, et al. (2003). Chicken DT40 cells stably transfected with the rat P2X7 receptor ion channel: a system suitable for the study of purine receptor-mediated cell death. *Biochem Pharmacol* 66: 415–424.
- Keystone EC, Wang MM, Layton M, Hollis S, McInnes IB (2012). Clinical evaluation of the efficacy of the P2X7

- purinergic receptor antagonist AZD9056 on the signs and symptoms of rheumatoid arthritis in patients with active disease despite treatment with methotrexate or sulphasalazine. *Ann Rheum Dis* 71: 1630–1635.
- Kim M, Jiang LH, Wilson HL, North RA, Surprenant A (2001). Proteomic and functional evidence for a P2X7 receptor signalling complex. *EMBO J* 20: 6347–6358.
- Kukley M, Schwan M, Fredholm BB, Dietrich D (2005). The role of extracellular adenosine in regulating mossy fiber synaptic plasticity. *J Neurosci* 25: 2832–2837.
- Labasi JM, Petrushova N, Donovan C, McCurdy S, Lira P, Payette MM, et al. (2002). Absence of the P2X7 receptor alters leukocyte function and attenuates an inflammatory response. *J Immunol* 168: 6436–6445.
- Le Feuvre RA, Brough D, Touzani O, Rothwell NJ (2003). Role of P2X7 receptors in ischemic and excitotoxic brain injury in vivo. *J Cereb Blood Flow Metab* 23: 381–384.
- Locovei S, Scemes E, Qiu F, Spray DC, Dahl G (2007). Pannexin1 is part of the pore forming unit of the P2X(7) receptor death complex. *FEBS Lett* 581: 483–488.
- Michel AD, Chessell IP, Hibell AD, Simon J, Humphrey PP (1998). Identification and characterization of an endogenous P2X7 (P2Z) receptor in CHO-K1 cells. *Br J Pharmacol* 125: 1194–1201.
- North RA (2002). Molecular physiology of P2X receptors. *Physiol Rev* 82: 1013–1067.
- Pankratov Y, Lalo U, Verkhatsky A, North RA (2006). Vesicular release of ATP at central synapses. *Pflugers Arch* 452: 589–597.
- Perelman A, Wachtel C, Cohen M, Haupt S, Shapiro H, Tzur A (2012). JC-1: alternative excitation wavelengths facilitate mitochondrial membrane potential cytometry. *Cell Death Dis* 3: e430.
- Pfeiffer ZA, Aga M, Prabhu U, Watters JJ, Hall DJ, Bertics PJ (2004). The nucleotide receptor P2X7 mediates actin reorganization and membrane blebbing in RAW 264.7 macrophages via p38 MAP kinase and Rho. *J Leukoc Biol* 75: 1173–1182.
- Ralevic V, Burnstock G (1998). Receptors for purines and pyrimidines. *Pharmacol Rev* 50: 413–492.
- Rassendren F, Buell GN, Virginio C, Collo G, North RA, Surprenant A (1997). The permeabilizing ATP receptor, P2X7. Cloning and expression of a human cDNA. *J Biol Chem* 272: 5482–5486.
- Rousseau DL Jr, Petrelli NJ, Kahlenberg MS (2004). Overview of anal cancer for the surgeon. *Surg Oncol Clin N Am* 13: 249–262.
- Ryu JK, Jantarotnotai N, Serrano-Perez MC, McGeer PL, McLarnon JG (2011). Block of purinergic P2X7R inhibits tumor growth in a C6 glioma brain tumor animal model. *J Neuropathol Exp Neurol* 70: 13–22.
- Schroder K, Tschopp J (2010). The inflammasomes. *Cell* 140: 821–832.
- Seeland S, Treiber A, Hafner M, Huwyler J (2011). On-line identification of P-glycoprotein substrates by monitoring of extracellular acidification and respiration rates in living cells. *Biochim Biophys Acta* 1808: 1827–1831.
- Seeland S, Torok M, Kettiger H, Treiber A, Hafner M, Huwyler J (2013). A cell-based, multiparametric sensor approach characterises drug-induced cytotoxicity in human liver HepG2 cells. *Toxicol In Vitro* 27: 1109–1120.
- Sharnez R, Lathia J, Kahlenberg D, Prabhu S, Dekleva M (2004). In situ monitoring of soil dissolution dynamics: a rapid and simple method for determining worst-case soils for cleaning validation. *PDA J Pharm Sci Technol* 58: 203–214.
- Skaper SD, Facci L, Culbert AA, Evans NA, Chessell I, Davis JB, et al. (2006). P2X(7) receptors on microglial cells mediate injury to cortical neurons in vitro. *Glia* 54: 234–242.
- Surprenant A (1996) Functional properties of native and cloned P2X receptors. *Ciba Found Symp* 198:208–219; discussion 219–222.
- Takenouchi T, Sekiyama K, Sekigawa A, Fujita M, Waragai M, Sugama S, et al. (2010). P2X7 receptor signaling pathway as a therapeutic target for neurodegenerative diseases. *Arch Immunol Ther Exp (Warsz)* 58: 91–96.
- Thedinga E, Kob A, Holst H, Keuer A, Drechsler S, Niendorf R, et al. (2007). Online monitoring of cell metabolism for studying pharmacodynamic effects. *Toxicol Appl Pharmacol* 220: 33–44.
- Volonte C, Amadio S, Cavaliere F, D'Ambrosi N, Vacca F, Bernardi G (2003). Extracellular ATP and neurodegeneration. *Curr Drug Targets CNS Neurol Disord* 2: 403–412.
- Volonte C, Apolloni S, Skaper SD, Burnstock G (2012). P2X7 receptors: channels, pores and more. *CNS Neurol Disord Drug Targets* 11: 705–721.
- Yoon MJ, Lee HJ, Kim JH, Kim DK (2006). Extracellular ATP induces apoptotic signaling in human monocyte leukemic cells, HL-60 and F-36P. *Arch Pharm Res* 29: 1032–1041.